JACS
JOURNAL OF THE AMERICAN CHEMICAL SOCIETY
Article
pubs.acs.org/JACS

"Brush-First" Method for the Parallel Synthesis of Photocleavable, Nitroxide-Labeled Poly(ethylene glycol) Star Polymers

Jenny Liu,[†,#] Alan O. Burts,[†,#] Yongjun Li,[‡] Aleksandr V. Zhukhovitskiy,[†] M. Francesca Ottaviani,[§] Nicholas J. Turro,[‡] and Jeremiah A. Johnson*[,†]

[†]Department of Chemistry, Massachusetts Institute of Technology, Cambridge, Massachusetts 02139, United States
[‡]Department of Chemistry, Columbia University, New York, New York 10027, United States
[§]Department of Earth, Life and Environment Sciences, University of Urbino, 61029 Urbino, Italy

Supporting Information

ABSTRACT: We describe the parallel, one-pot synthesis of core-photocleavable, poly(norbornene)-*co*-poly(ethylene glycol) (PEG) brush-arm star polymers (BASPs) via a route that combines the "graft-through" and "arm-first" methodologies for brush polymer and star polymer synthesis, respectively. In this method, ring-opening metathesis polymerization of a norbornene–PEG macromonomer generates small living brush initiators. Transfer of various amounts of this brush initiator to vials containing a photocleavable bis-norbornene cross-linker yielded a series of water-soluble BASPs with low polydispersities and molecular weights that increased geometrically as a function of the amount of bis-norbornene added. The BASP cores were cleaved upon exposure to UV light; the extent of photo-disassembly depended on the amount of cross-linker. EPR spectroscopy of nitroxide-labeled BASPs was used to probe differences between the BASP core and surface environments. We expect that BASPs will find applications as easy-to-synthesize, stimuli-responsive core–shell nanostructures.

INTRODUCTION

The advent of efficient, functional-group-tolerant polymerization reactions has revolutionized the synthesis of tailored macromolecules with precisely defined nanoscopic features.[1,2] Ring-opening metathesis polymerization (ROMP) is one of the most powerful ways to make functional polymers in a controlled fashion.[3−5] Recently, ROMP catalyzed by third-generation Grubbs catalyst[6] (**1**) has been applied to the synthesis of bottle-brush,[7−9] bivalent-bottle-brush,[10−13] and dendronized polymers[14] via a "graft-through" strategy whereby functional norbornene macromomoners (MMs) are polymerized directly. The synthesis of functional polymeric nanostructures can be greatly simplified via the graft-through approach: all the functionality of the desired nanostructure can be built into MMs.[15] Graft-through polymerization of these multifunctional MMs generates polymers of tunable size and functionality for screening in an application of interest. Inefficient polymer modification reactions are avoided; synthetic efficiency is increased.

In this report, we seek to broaden the utility of graft-through polymerization via combination with the arm-first technique for star polymer synthesis.[16−18] In a typical arm-first polymerization, linear, end-functional polymers (i.e., "arms") are cross-linked via copolymerization with a multifunctional monomer or "cross-linker."[17] Cross-linking can be initiated between preformed, end-functional macroinitiators (MIs), MMs, or *in situ* between living polymer chains. The arm-first method was first used in the context of anionic polymerization,[16,17] and has since been applied to a number of controlled radical polymerization processes[18−33] and ROMP.[34−37] Regardless of the polymerization method used, the mechanism of star formation involves a balance of kinetically limited "star+star" and "star+linear" coupling reactions that ultimately defines the structure, size, and uniformity of the final star product.[38]

In a pair of seminal reports,[34,35] Schrock and co-workers showed that addition of bis-olefin cross-linkers to living ROMP reactions led to poly(norbornene)-based star polymers with low polydispersities (PDIs) and ∼20−175 kDa molecular weights (MWs). This basic strategy has since been employed for the preparation of a wide array of functional materials. For example, Buchmeiser has reported several bis-olefin cross-linked "polymer monoliths" whose functionalities are defined by the choice of monomers and cross-linkers.[39−47] These microparticulate materials have myriad applications as scaffolds for tissue engineering, separation media, and supported catalysis.

Otani has used Schrock's Mo(CHCMe$_2$Ph)(N-2,6-^{i}Pr$_2$C$_6$H$_3$)(O^{t}Bu)$_2$ catalyst to initiate ROMP of norbornene followed by addition of a bis-olefin cross-linker to generate poly(norbornene) stars with masses approaching 200 kDa and

Received: July 10, 2012
Revised: September 5, 2012
Published: September 6, 2012

   dx.doi.org/10.1021/ja3067176 | *J. Am. Chem. Soc.* 2012, 134, 16337−16344

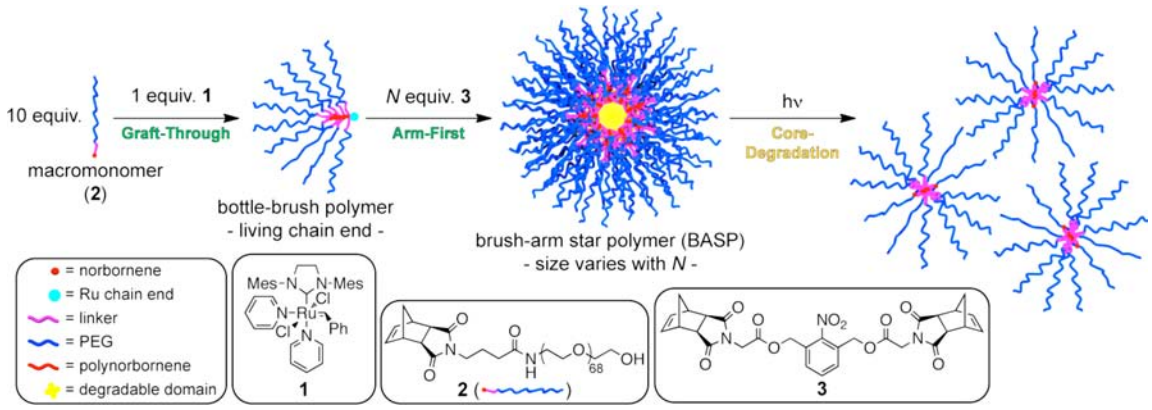

Figure 1. Synthesis of poly(ethylene glycol) brush-arm star polymers via graft-through ring-opening metathesis polymerization of macromomoner **2** initiated by **1**, followed by arm-first cross-linking with **3**. The nitrobenzyloxycarbonyl cores of these BASPs degrade under ultraviolet light.

PDI values ranging from ~1.2 to 1.5.[37] In this work, another portion of monomer was added after cross-linking to initiate linear polymer growth from the star cores followed by surface functionalization with aldehyde derivatives via a Wittig-like chain transfer process. The same group later used this approach to generate glycosylated star polymers with terminal fluorophores via use of a norbornene–galactose monomer and quenching with pyrenecarboxaldehyde.[36] Nomura recently reported the synthesis of oligo(thiophene)-[48] and pyridine-coated[49] star polymers via this same multistep strategy.

The above-mentioned arm-first ROMP examples are related in that they utilize small-molecule monomers to generate MIs, which are ultimately cross-linked to form star polymers. As a result, the ratio of star arms to initiation sites (defined here as m) equals 1 during the key star formation process (the final value of m becomes 2 if a second monomer is added to initiate arm growth from the core). In related arm-first atom transfer radical polymerization (ATRP) reactions, Matyjaszewski and co-workers have shown that increasing m via use of MMs and small molecule initiators rather than MIs reduces star+star coupling and leads to more homogeneous star polymer products.[50] Subsequent work from the Matyjaszewski group has shown that this basic concept is quite general for arm-first ATRP; several impressive, multifunctional star polymers have been prepared via arm-first ATRP coupling of MMs.[18,22,51,52]

To our knowledge, arm-first MM cross-linking has not been applied in the context of ROMP. In principle, this strategy would enable synthesis of multifunctional star polymers bearing moieties that are incompatible with radical polymerization mechanisms (e.g., persistent radicals like nitroxides). Furthermore, surface- or core-functionalized star polymers and miktoarm star polymers could be prepared via arm-first cross-linking of appropriate telechelic or branched MMs.[10−13,53]

RESULTS AND DISCUSSION

In Matyjaszewski's work, (meth)acrylate-terminated MMs, an alkyl bromide initiator, cross-linker (e.g., divinylbenzene), and copper catalyst are typically combined at the outset of polymerization. As a result, star cores are formed rapidly via a statistical combination of star+star and star+linear reactions between MM, cross-linker, and newly formed stars. *Unreacted MM is always present in the reaction medium.* At later stages of the reaction, when large star polymers have formed, the rate of star+star coupling is diminished due to steric interactions and the only viable star growth pathway is chain-like star+linear coupling between unreacted MMs and living star cores.

When we attempted the same method in the context of ROMP using poly(ethylene glycol) (PEG) MM **2** and photocleavable cross-linker **3** (Figure 1) we invariably obtained materials with very high MW and PDI values (Figure S1). This result suggested that ROMP of **3** was too fast to afford control over the arm-first process; **2** was not incorporated into the growing star polymer quickly enough to preclude rapid cross-linking.

We envisioned an alternative approach to controlling m: rather than combine MM and cross-linker at the outset, it should be possible to grow short, living "brush initiators" (BIs) via homopolymerization of MM (Figure 1, first step), followed by addition of N equiv of cross-linker (Figure 1, second step) to generate star polymers wherein the star polymer arms are themselves brush polymers (i.e., "brush-arm star polymers", or BASPs). In this novel approach, m is the degree of polymerization of the BI, and there is no free MM in the reaction mixture; star growth can only occur via star+star coupling.

Here we demonstrate that this "brush-first" strategy is useful for the parallel synthesis of degradable PEG BASPs over a wide range of nanoscopic sizes with tunable surface and core functionalities. We uncover a novel geometric star growth mechanism that yields homogeneous BASPs whose sizes depend on the brush length (m) and the amount of cross-linker (N). We demonstrate that surface and core functionalization can be readily achieved via use of telechelic or branched MMs, respectively: subsequent chain transfer or growth of new arms is not required. Furthermore, use of a photocleavable cross-linker (e.g., **3**) facilitates BASP degradation in response to UV light (Figure 1, third step). This unique combination of synthetic ease and functional versatility will make brush-first BASP synthesis a broadly useful methodology for nanoparticle synthesis.

Synthesis of BASPs. To test the viability of brush-first BASP synthesis via ROMP, 1 equiv of catalyst **1** was added to 10 equiv of MM **2** in tetrahydrofuran (THF) to form a living brush initiator with DP = 10. After complete consumption of **2**, ~10 min, aliquots of the polymerization mixture were added to vials that contained 10, 15, and 20 equiv of cross-linker **3**. After 4 h the reactions were quenched with ethyl vinyl ether, and solvent was removed *in vacuo*.

dx.doi.org/10.1021/ja3067176 | J. Am. Chem. Soc. 2012, 134, 16337−16344

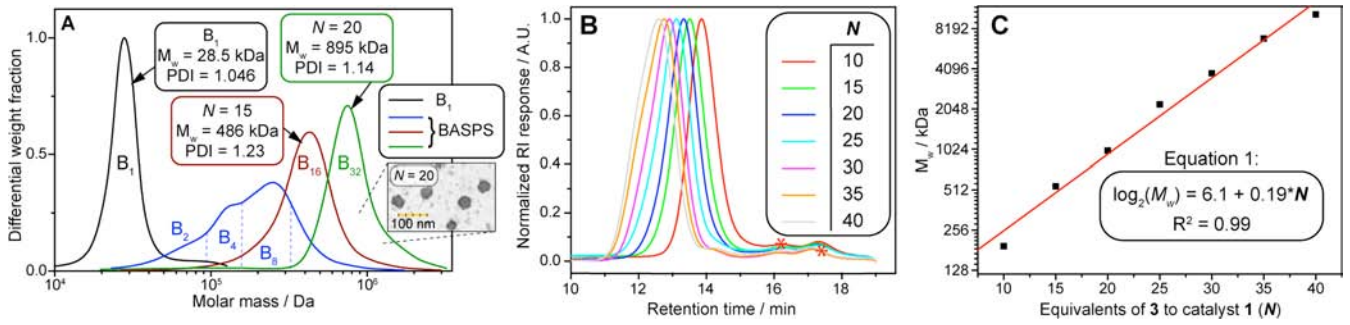

Figure 2. (A) Differential mass GPC traces of N = 10, 15, and 20 BASPs after 4 h cross-linking in THF. Inset: transmission electron micrograph of N = 20 BASP. (B) Refractive index GPC traces for BASPs with N = 10–40. Unreacted MM and B_1 are labeled with red asterisks. M_w values increased geometrically with N. (C) Log_2 plot of M_w versus N for the BASP series from part B. Linear fitting produces Equation 1, which relates BASP M_w to N.

The absolute MW of each crude BASP was obtained by gel permeation chromatography (GPC) coupled with a multiangle laser light scattering (MALLS) detector. Figure 2A shows differential weight fraction plots for the set of N = 10, 15, and 20 BASPs. As expected, the brush initiator (B_1) possessed a low PDI and a weight-average molecular weight (M_w) of 28.5 kDa (DP ≈ 9, black trace). The N = 10 sample showed multiple mass distributions. The N = 15 and N = 20 samples possessed monomodal MW distributions with M_w values corresponding to ~B_{16} and ~B_{32}, respectively. As N increased by 5, the M_w of the resulting BASP doubled.

Intrigued by these results, we next examined a wider range of N values and an alternative ROMP solvent (CH_2Cl_2, DCM) to verify if this observed mass doubling was reproducible over a wider range of N under varied conditions. Brush-first reactions were performed with N values ranging from 10 to 40 in increments of 5. Cross-linking was allowed to proceed for 6 h to ensure maximal conversion. GPC analysis of the crude BASPs showed monomodal MW distributions for all N values tested (Figure 2B), and very high conversions (unreacted **2** and B_1, marked with red asterisks in Figure 2B, were present in less than 3% for all cases). The M_w values for this series ranged from 149 kDa (when N = 10) to 8.11 MDa (when N = 40). With each increase of N by five, the BASP M_w doubled; a log_2 plot of M_w versus N is linear (Figure 2C). Fitting of these data provides Equation 1, which allows prediction of M_w given N for this system.

Mechanistic hypothesis. To explain the observed geometric MW increase we propose the mechanism depicted in Figure 3. In stage I (Figure 3A), graft-through polymerization generates a living brush polymer with DP = m. Addition of N equiv of cross-linker gives a living "primary brush initiator" (B_1). In contrast to the Matyjaszewski method, *the MM is consumed in the graft-through step*; the ratio of arms to initiator is large (m), but *the only remaining reaction pathway for B_1 is star–star coupling* (stage II, Figure 3B). If all BASPs, B_x, couple with equal affinity the reaction is classical step-growth; the PDI approaches 2.0 with conversion.[54] Low PDIs can be obtained if BASP coupling is inhibited with increased size.[55,56] In stage II, B_1+B_1 coupling to generate dimer B_2 is the most viable reaction from a kinetic standpoint. If $k_{1+2} \ll k_{1+1}$ then the reaction mixture will contain a larger than statistical fraction of B_2, B_1 will be consumed, and B_3 will be suppressed. Transport limitations, steric hindrance, and/or intramolecular norbornene consumption can all contribute to making $k_{1+2} \ll k_{1+1}$.

At the end of stage II the core of B_2 still contains living initiators and norbornene groups that could couple at longer

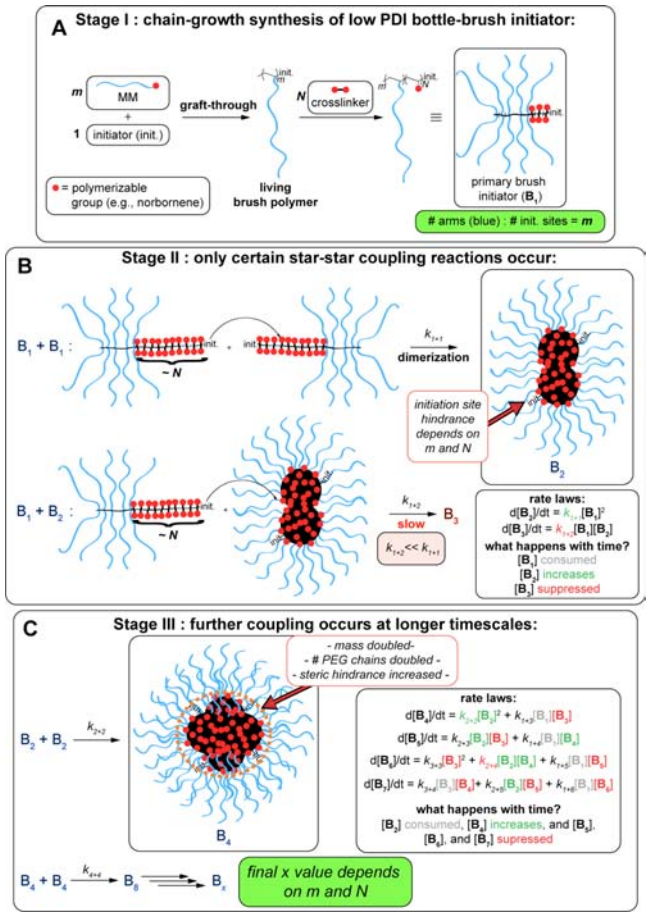

Figure 3. Proposed mechanism for geometric BASP formation via the "brush-first" method.

time scales. Figure 3C lists rate laws for formation of B_4, B_5, B_6, and B_7. Since B_2 is the major product in stage II, bimolecular B_2+B_2 coupling to form B_4 is the most viable reaction (stage III, Figure 3C). Formation of other B_x values is suppressed due to low concentrations of the required B_1 or B_3 coupling partners or unfavorable rate constants (e.g., $k_{2+4} \ll k_{2+2}$). In general, if $k_{x+x} \gg k_{x+2x}$, iterative dimerization at increasingly long time scales can continue until a final persistent value of x is reached.

It should be noted that 100% dimerization for real systems is unlikely, especially at the earliest stages of the BASP formation process. The proposed mechanism is an idealized description that would lead to BASPs with low PDI and geometric mass

dx.doi.org/10.1021/ja3067176 | J. Am. Chem. Soc. 2012, 134, 16337–16344

increase. Of course, some B_3 will form during stage II, and a corresponding fraction of "non-dimerized" x values B_5, B_6, etc.. will form in stage III. The key is finding conditions that will maximize formation of dimerized products, and in turn yield homogeneous star polymers.

Schrock noted that the use of linear MIs leads to statistical formation of stars during early stages of arm-first ROMP reactions with small monomers (i.e., equal amounts of B_1, B_2, B_3, etc.).[35] This result suggests that linear MIs are not hindered enough to provide conditions where $k_{x+x} \gg k_{x+2x}$. We hypothesize that the steric bulk of brush polymer arms obtained via the brush-first method is key to the observed geometric growth. However, this growth mechanism may be operative in many of the arm-first polymerization examples described in the preceding section. These reports never explored a wide range of N values. Perhaps iterative dimerization was simply overlooked.

Mechanistic Studies. If the mechanism proposed in Figure 3 were operative, one would predict that the final values of x for a given BASP would depend on both N and m. In particular, if N is increased, the number of available cross-linking sites increases and the overall length of the cross-linker block of B_1 increases. These features should increase the BASP core size, reduce steric hindrance, and allow access to larger x values. This trend is evident in Figure 2.

In contrast, as brush length (m) are increased we expect that the final BASP x value should decrease due to increased steric hindrance. Figure 4A–C shows GPC traces for BASPs formed

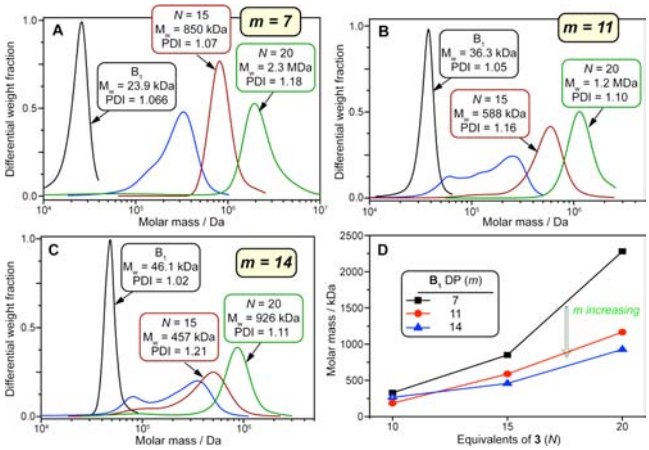

Figure 4. (A–C) GPC traces for m = 7, 11, and 14 BASPs with N = 10, 15, and 20. (D) Plot of M_w versus N for various m values. As m increases, the final size of the BASP decreases.

under conditions identical to those used in Figure 2A (THF solvent, 4 h cross-linking) using N = 10, 15, and 20 and m = 7, 11, and 14. The N = 10 sample for each m value (blue traces) was multimodal suggesting that 10 equiv of **3** are not sufficient to afford control in this system. However, uniform BASPs were obtained for nearly every N = 15 and N = 20 sample, regardless of m. A plot of M_w versus N for the various m values tested shows that as m increases, the BASP mass decreases. When m = 7 and N = 20, B_{64} is obtained. When m is increased to 11 or 14, with N held at 20, B_{32} is obtained. The same trend holds for the N = 15 cases. These results demonstrate that decreasing m allows for further dimerization events; smaller B_1 species lead to larger BASPs.

Next we performed kinetic analyses for N = 15 and 20 (m = 10) BASP formation reactions. For these studies, small samples were taken from a cross-linking reaction, quenched with ethyl vinyl ether, and directly analyzed by GPC. If the mechanism from Figure 3 is correct, it should be possible to trap various dimerized B_x products over the course of the cross-linking reaction. Furthermore, B_1 should be consumed at early stages of the reaction. The results for the N = 15 case are shown in Figure 5A. After 9 min (red trace) there is a convoluted mixture

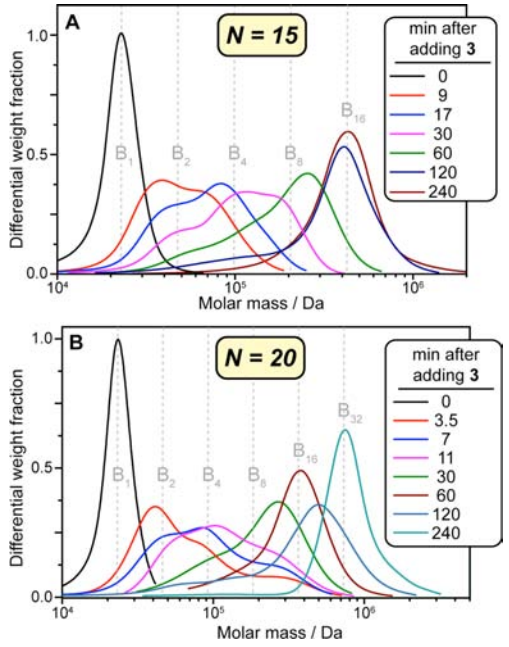

Figure 5. Kinetic analysis of BASP formation. Dimerized B_x species are clearly visible throughout the cross-linking reaction. N determines the final average x value.

of B_x values that contains B_1 and B_2 fractions, along with some B_3 and B_4. After 30 min (purple trace), B_1 is completely consumed and peaks for B_2, B_4, and B_8 are clearly visible as major components. After 240 min these smaller B_x values converge to give product enriched with B_{16}.

In the N = 20 case (Figure 5B), dimerized products are observed in the earliest time point (3.5 min), and B_1 is consumed within 11 min. It appears that increasing N leads to faster cross-linking in earlier stages, which supports the hypothesis that increased N reduces steric hindrance. Here, at 60 min (maroon trace) the system consists almost entirely of B_{16} (240 min needed for the N = 15 case). After 120 min, there is a ~1:1 mixture of B_{16} and B_{32}; after 240 min, only B_{32} is observed. GPC analysis of both reactions after 24 h showed no increase in mass or change in PDI. Taken together, these data provide strong support for the mechanism depicted in Figure 3. Iterative dimerization events occur until the reaction system settles on an optimal persistent x value.

BASP Degradation Studies. Cross-linker **3** possesses a nitrobenzyloxycarbonyl (NBOC) group known to cleave upon UV irradiation.[57] The concept of embedding NBOC groups within polymeric structures has become a common strategy for the synthesis of photodegradable materials.[58−61] As described in Figure 1, complete cleavage of NBOC groups in the core of BASPs should regenerate the parent brush polymers with short

dx.doi.org/10.1021/ja3067176 | J. Am. Chem. Soc. 2012, 134, 16337−16344

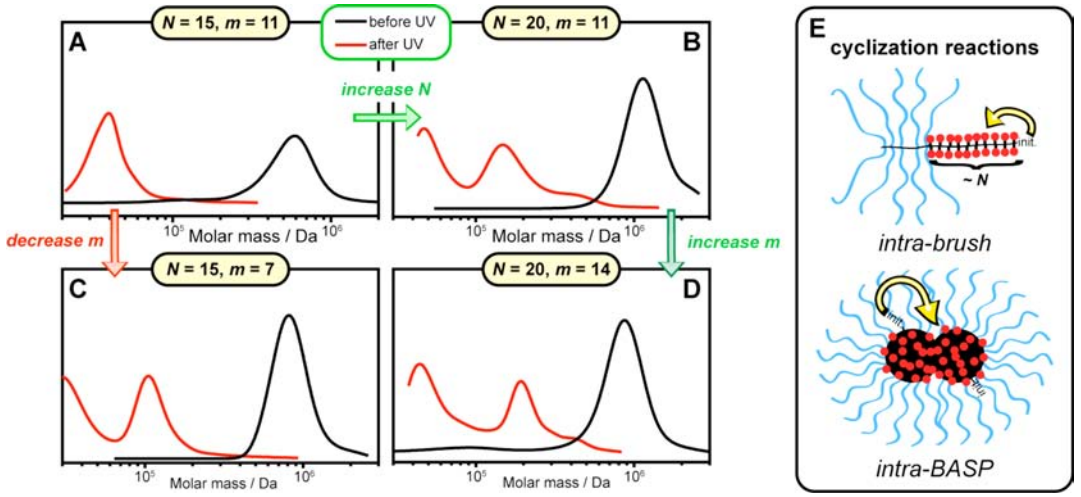

Figure 6. (A–D) GPC analysis of BASP degradation for a variety of *N* and *m* values. (E) Possible intramolecular cyclization reactions that increase the number of NBOC groups that must be cleaved for complete BASP degradation.

blocks of NBOC cleavage products appended to the chain ends (the latter are neglected in Figure 3 for clarity).

Figure 6 shows GPC traces of various BASPs before and after UV irradiation (365 nm for 4 h in THF). In the $N = 15$, $m = 11$ case the degradation reaction regenerates the parent brush polymer cleanly (Figure 6A). However, when *N* is increased to 20 and *m* held constant at 11 (Figure 6B), a mixture of B_x cleavage products is obtained; degradation does not reach 100% conversion. Similar results were obtained when *N* was held at 15 and *m* decreased to 7 (Figure 6C), and when both *m* and *N* were increased (Figure 6D). As described in the previous section, increasing *N* and decreasing *m* both led to larger BASPs. The BASP samples studied in Figure 6A–D have M_w values of 588 (B_{16}), 1.2 (B_{32}), 850 (B_{32}), and 926 kDa (B_{16}), respectively. Given the B_x value for each sample, the number of NBOC groups per BASP can be easily calculated as $N \times B_x$; the BASP from Figure 6A has ~240 NBOC groups, while the BASPs from Figure 6B–D have 640, 480, and 320 NBOC groups, respectively.

We hypothesize that this variation in the number of NBOC groups per BASP defines the overall extent of degradation. Only the sample with the fewest NBOC groups reached complete degradation. Cyclization reactions—i.e., intramolecular cross-linking between Ru and unreacted norbornene groups within the same brush or BASP core (Figure 6E)—are likely to occur. Photocleavage of these intramolecular cross-links would not lead to a decrease in mass, but instead would manifest itself as an apparent mass increase by GPC due to increased hydrodynamic volume post-cleavage.[62,63]

As the number of NBOC moieties increases in a given BASP, the number of intramolecular cross-links increases as well. Though NBOC cleavage is generally a very efficient reaction, there appears to be a limit to the number of NBOC groups that can be successfully cleaved in a single BASP particle. This limit may be due to a small percentage of side reactions that consume NBOC groups but do not lead to cleavage, or competing light absorption between unreacted NBOC groups and nitrosobenzaldehyde cleavage products.

Transmission electron microscopy (TEM) images of $N = 15$ and 20 ($m = 14$) BASPs before and after irradiation (Figure 7) agree with the GPC results from Figure 6. Figure 7A shows the $N = 20$ particles. UV irradiation for 30 min in H_2O led to a

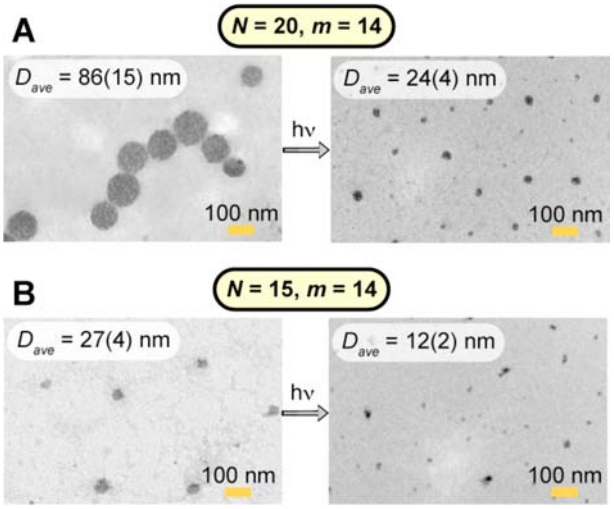

Figure 7. TEM images of BASPs before and after UV irradiation.

decrease in size from 86 to 24 nm. For the $N = 15$ case (Figure 7B), the starting particles were much smaller (27 nm), and irradiation led to formation of 12 nm particles.

Dynamic light-scattering (DLS) was also used to study photoinitiated BASP disassembly. Irradiation of aqueous BASP solutions for 10 min led to observed decreases in hydrodynamic diameter, D_h. The $N = 15$ BASP had $D_h = 24$ nm before irradiation (green histogram, Figure 8), while irradiation yielded 8 nm particles. In the $N = 40$ case, 28 nm degradation products are obtained.

These BASP particles are highly soluble in water, and they do not aggregate significantly with time. However, BASPs of similar M_w always appear larger by TEM than DLS. This observation may be due to the fact that the BASP core is very hydrophobic; the BASP structure is collapsed in water to avoid interactions between the core and the solvent.

To probe this hypothesis in more detail, and demonstrate that surface and core functional BASPs could be easily generated in one pot, 5% of nitroxide-labeled MMs **4** and **5** were incorporated into BASPs with $N = 15$ (Figure 9). Use of telechelic MM **4** leads to nitroxide groups at the BASP surface while use of branched MM **5** leads to BASPs with core-bound

dx.doi.org/10.1021/ja3067176 | J. Am. Chem. Soc. 2012, 134, 16337–16344

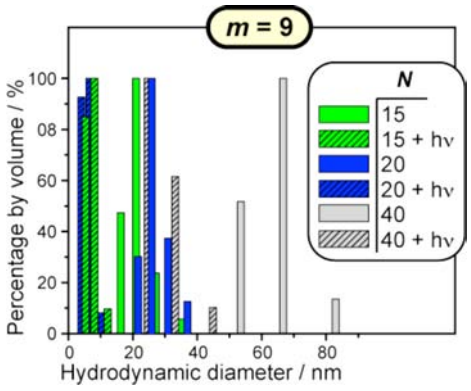

Figure 8. Aqueous volume-average dynamic light-scattering histograms before and after BASP degradation. DLS correlation functions were fitted using the CONTIN algorithm.

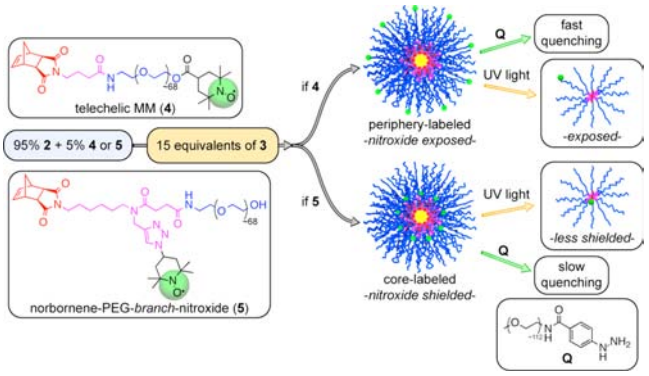

Figure 9. Nitroxide MMs **4** and **5** allow for selective periphery and core BASP labeling, respectively. The rate of nitroxide quenching with PEG-PhNHNH$_2$ depends on the nitroxide location within the BASP nanostructure.

nitroxides. The GPC traces for both the peripherally-labeled (**p**) and core-labeled (**c**) samples indicated very high MM conversion and monomodal MW distributions (Figure 10A); the use of nitroxides and branched MMs does not inhibit BASP formation. DLS analysis confirms that the hydrodynamic radii of **p** and **c** decrease under UV irradiation (Figure 10B).

Electron paramagnetic resonance (EPR) spectroscopy is a convenient method for studying nitroxide-labeled macromolecular systems; the EPR spectrum is sensitive to environmental factors such as polarity, viscosity, and steric hindrance.[53,64,65] Figure 10C shows EPR spectra for BASPs **c** and **p** before and after irradiation. The increased spectral broadening for **c** compared to **p** is indicative of the hindered environment experienced by the core-bound nitroxide label. This steric hindrance is captured quantitatively by an increased correlation time for rotational diffusion, τ, which is 0.03 ns for **p** and 0.95 ns for **c**. UV degradation leads to no change in the spectrum for **p**; a small but significant sharpening (labeled with an asterisk in Figure 10C) is observed for **c**. These results suggest that nitroxides at the BASP surface are equally shielded before and after degradation while core nitroxides experience less steric hindrance after irradiation (depicted schematically in Figure 9).

EPR active nitroxides are reduced by phenyl hydrazine derivatives to generate EPR silent hydroxylamines. This reaction "quenches" the EPR signals; the rate of quenching depends on the steric hindrance experienced by the hydrazine

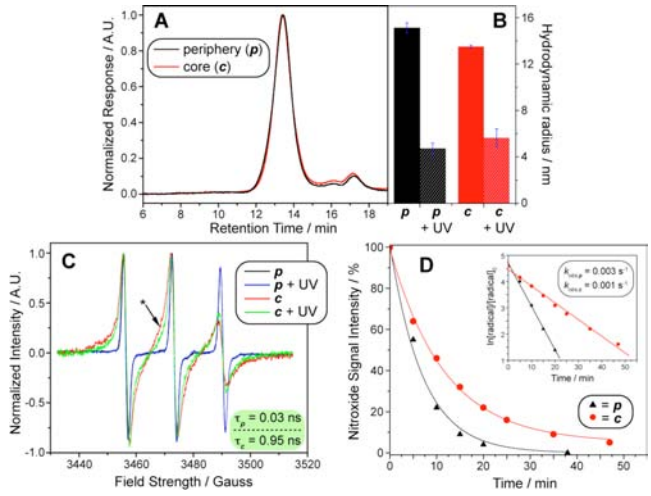

Figure 10. (A) Gel permeation chromatography traces for peripherally (**p**) and core (**c**)-labeled BASPs. (B) Dynamic light-scattering analysis of **p** and **c**. (C) Electron paramagnetic resonance spectra before and after UV irradiation. (D) Quenching kinetics.

reagent. We previously demonstrated that quenching rates are faster for peripherally-labeled poly(lactide) brush polymers in organic solvents compared to core-labeled analogues.[53] Here we describe the first application of this method to aqueous BASP systems. To explore quenching under these conditions, water-soluble, polymeric quencher **Q** was designed (Figure 9). Quenching was performed under pseudo-first-order conditions with excess **Q**. We found that quenching of the EPR signal of surface-labeled **p** was 3 times faster than for core-labeled **c**, which confirms that the BASP core is sterically shielded from external reagents (Figure 10D). Shielding of hydrophobic materials within a star or dendritic core has been exploited for one-pot dual catalysis[66] and drug delivery applications.[67,68] Ongoing studies are aimed toward using nitroxide-labeled BASPs as supported oxidation catalysts.

This work represents the first demonstration of brush-first cross-linking to give brush-arm star polymers. The presented poly(ethylene glycol) BASPs grow geometrically with increased cross-linker amount, which allows facile access to nanoparticles with a wide range of diameters. UV irradiation leads to rapid BASP degradation; the overall extent of degradation depends on the number of nitrobenzyloxycarbonyl groups in the BASP core. The functional group tolerance of catalyst **1** was exploited for the synthesis of nitroxide-labeled BASPs. EPR analysis confirmed that the BASP core and periphery have different environmental features and reactivity. We are currently applying this novel "brush-first" method for the one-pot parallel synthesis of multifunctional nanostructures for a variety of applications.

■ ASSOCIATED CONTENT

Ⓢ Supporting Information

Supplemental figures, details regarding EPR analysis, detailed synthetic procedures and spectral data. This material is available free of charge via the Internet at http://pubs.acs.org.

■ AUTHOR INFORMATION

Corresponding Author

jaj2109@mit.edu

Author Contributions

[#]J.L. and A.O.B. contributed equally to this work.

Notes

The authors declare no competing financial interest.

■ ACKNOWLEDGMENTS

We thank the Massachusetts Institute of Technology Department of Chemistry and the DoD NDSEG program (graduate fellowship for A.V.Z.) for support of this work. We also thank Dr. P. Patel for advice related to preparation of **Q**, and Prof. M. Movassaghi for use of his group's Rayonet photoreactor.

■ REFERENCES

(1) Hawker, C. J.; Wooley, K. L. *Science* **2005**, *309*, 1200−1205.
(2) Yagci, Y.; Tasdelen, M. A. *Prog. Polym. Sci.* **2006**, *31*, 1133−1170.
(3) *Handbook of Metathesis*; Wiley-VCH: Weinheim, 2003; Vol. 3.
(4) Bielawski, C. W.; Grubbs, R. H. *Prog. Polym. Sci.* **2007**, *32*, 1−29.
(5) Leitgeb, A.; Wappel, J.; Slugovc, C. *Polymer* **2010**, *51*, 2927−2946.
(6) Love, J. A.; Morgan, J. P.; Trnka, T. M.; Grubbs, R. H. *Angew. Chem., Int. Ed.* **2002**, *41*, 4035−4037.
(7) Xia, Y.; Kornfield, J. A.; Grubbs, R. H. *Macromolecules* **2009**, *42*, 3761−3766.
(8) Li, Z.; Zhang, K.; Ma, J.; Cheng, C.; Wooley, K. L. *J. Polym. Sci., Part A: Polym. Chem.* **2009**, *47*, 5557−5563.
(9) Le, D.; Montembault, V.; Soutif, J. C.; Rutnakornpituk, M.; Fontaine, L. *Macromolecules* **2010**, *43*, 5611−5617.
(10) Johnson, J. A.; Lu, Y.-Y.; Burts, A. O.; Lim, Y.-H.; Finn, M. G.; Koberstein, J. T.; Turro, N. J.; Tirrell, D. A.; Grubbs, R. H. *J. Am. Chem. Soc.* **2011**, *133*, 559−566.
(11) Johnson, J. A.; Lu, Y. Y.; Burts, A. O.; Xia, Y.; Durrell, A. C.; Tirrell, D. A.; Grubbs, R. H. *Macromolecules* **2010**, *43*, 10326−10335.
(12) Li, Y. K.; Zou, J.; Das, B. P.; Tsianou, M.; Cheng, C. *Macromolecules* **2012**, *45*, 4623−4629.
(13) Li, Y.; Themistou, E.; Zou, J.; Das, B. P.; Tsianou, M.; Cheng, C. *ACS Macro Lett.* **2012**, *1*, 52−56.
(14) Boydston, A. J.; Holcombe, T. W.; Unruh, D. A.; Frechet, J. M. J.; Grubbs, R. H. *J. Am. Chem. Soc.* **2009**, *131*, 5388−5389.
(15) Hadjichristidis, N.; Pitsikalis, M.; Iatrou, H.; Pispas, S. *Macromol. Rapid Commun.* **2003**, *24*, 979−1013.
(16) Kohler, A.; Koessler, I.; Zilliox, J. G.; Polacek, J.; Rempp, P. *Eur. Polym. J.* **1972**, *8*, 627.
(17) Worsfold, D. J.; Zilliox, J. G.; Rempp, P. *Can. J. Chem.* **1969**, *47*, 3379
(18) Matyjaszewski, K.; Tsarevsky, N. V. *Nature Chem.* **2009**, *1*, 276−288.
(19) Xia, J. H.; Zhang, X.; Matyjaszewski, K. *Macromolecules* **1999**, *32*, 4482−4484.
(20) Gao, H. F.; Matyjaszewski, K. *Macromolecules* **2006**, *39*, 3154−3160.
(21) Gao, H.; Matyjaszewski, K. *J. Am. Chem. Soc.* **2007**, *129*, 11828−11834.
(22) Gao, H. F.; Matyjaszewski, K. *Macromolecules* **2008**, *41*, 4250−4257.
(23) Dai, F. Y.; Sun, P.; Liu, Y. J.; Liu, W. G. *Biomaterials* **2010**, *31*, 559−569.
(24) Goh, T. K.; Yamashita, S.; Satoh, K.; Blencowe, A.; Kamigaito, M.; Qiao, G. G. *Macromol. Rapid Commun.* **2011**, *32*, 456−461.
(25) Koda, Y.; Terashima, T.; Nomura, A.; Ouchi, M.; Sawamoto, M. *Macromolecules* **2011**, *44*, 4574−4578.
(26) Terashima, T.; Motokawa, R.; Koizumi, S.; Sawamoto, M.; Kamigaito, M.; Ando, T.; Hashimoto, T. *Macromolecules* **2010**, *43*, 8218−8232.
(27) Gao, H. F.; Tsarevsky, N. V.; Matyjaszewski, K. *Macromolecules* **2005**, *38*, 5995−6004.
(28) Bosman, A. W.; Vestberg, R.; Heumann, A.; Frechet, J. M. J.; Hawker, C. J. *J. Am. Chem. Soc.* **2003**, *125*, 715−728.
(29) Bosman, A. W.; Heumann, A.; Klaerner, G.; Benoit, D.; Frechet, J. M. J.; Hawker, C. J. *J. Am. Chem. Soc.* **2001**, *123*, 6461−6462.
(30) Adkins, C. T.; Harth, E. *Macromolecules* **2008**, *41*, 3472−3480.
(31) Cheng, F.; Bonder, E. M.; Doshi, A.; Jakle, F. *Polym. Chem.* **2012**, *3*, 596−600.
(32) Zheng, G. H.; Pan, C. Y. *Polymer* **2005**, *46*, 2802−2810.
(33) Blencowe, A.; Tan, J. F.; Goh, T. K.; Qiao, G. G. *Polymer* **2009**, *50*, 5−32.
(34) Saunders, R. S.; Cohen, R. E.; Wong, S. J.; Schrock, R. R. *Macromolecules* **1992**, *25*, 2055−2057.
(35) Bazan, G. C.; Schrock, R. R. *Macromolecules* **1991**, *24*, 817−823.
(36) Otani, H.; Fujita, S.; Watanabe, Y.; Fujiki, M.; Nomura, K. *Macromol. Symp.* **2010**, *293*, 53−57.
(37) Nomura, K.; Watanabe, Y.; Fujita, S.; Fujiki, M.; Otani, H. *Macromolecules* **2009**, *42*, 899−901.
(38) Gao, H. F. *Macromol. Rapid Commun.* **2012**, *33*, 722−734.
(39) Bandari, R.; Buchmeiser, M. R. *Catal. Sci. Technol.* **2012**, *2*, 220−226.
(40) Weichelt, F.; Lenz, S.; Tiede, S.; Reinhardt, I.; Frerich, B.; Buchmeiser, M. R. *Beilstein J. Org. Chem.* **2010**, *6*, 1199−1205 (No. 1137)..
(41) Weichelt, F.; Frerich, B.; Lenz, S.; Tiede, S.; Buchmeiser, M. R. *Macromol. Rapid Commun.* **2010**, *31*, 1540−1545.
(42) Mayr, M.; Mayr, B.; Buchmeiser, M. R. *Angew. Chem., Int. Ed.* **2001**, *40*, 3839−3842.
(43) Buchmeiser, M. R.; Kroll, R.; Wurst, K.; Schareina, T.; Kempe, R.; Eschbaumer, C.; Schubert, U. S. *Macromol. Symp.* **2001**, *164*, 187−196.
(44) Buchmeiser, M. R.; Wurst, K. *J. Am. Chem. Soc.* **1999**, *121*, 11101−11107.
(45) Sinner, F.; Buchmeiser, M. R.; Tessadri, R.; Mupa, M.; Wurst, K.; Bonn, G. K. *J. Am. Chem. Soc.* **1998**, *120*, 2790−2797.
(46) Buchmeiser, M. R.; Seeber, G.; Bonn, G. K.; Bertsch, T. *J. Chromatogr., A* **1998**, *809*, 121−129.
(47) Buchmeiser, M. R.; Atzl, N.; Bonn, G. K. *J. Am. Chem. Soc.* **1997**, *119*, 9166−9174.
(48) Takamizu, K.; Nomura, K. *J. Am. Chem. Soc.* **2012**, *134*, 7892−7895.
(49) Nomura, K.; Tanaka, K.; Fujita, S. *Organometallics* **2012**, *31*, 5074−5080.
(50) Gao, H. F.; Ohno, S.; Matyjaszewski, K. *J. Am. Chem. Soc.* **2006**, *128*, 15111−15113.
(51) Matyjaszewski, K.; Cho, H. Y.; Gao, H. F.; Srinivasan, A.; Hong, J.; Bencherif, S. A.; Siegwart, D. J.; Paik, H. J.; Hollinger, J. O. *Biomacromolecules* **2010**, *11*, 2199−2203.
(52) Gao, H. F.; Matyjaszewski, K. *Macromolecules* **2007**, *40*, 399−401.
(53) Xia, Y.; Li, Y. J.; Burts, A. O.; Ottaviani, M. F.; Tirrell, D. A.; Johnson, J. A.; Turro, N. J.; Grubbs, R. H. *J. Am. Chem. Soc.* **2011**, *133*, 19953−19959.
(54) Flory, P. J. *Principles of Polymer Chemistry*; Cornell University Press: Ithaca, NY, 1953
(55) Nanda, V. S.; Jain, S. C. *J. Chem. Phys.* **1968**, *49*, 1318−1320.
(56) Cotts, D. B.; Berry, G. C. *Macromolecules* **1981**, *14*, 930−934.
(57) Bochet, C. G. *J. Chem. Soc., Perkin Trans. 1* **2002**, 125−142.
(58) Johnson, J. A.; Baskin, J. M.; Bertozzi, C. R.; Koberstein, J. T.; Turro, N. J. *Chem. Commun.* **2008**, 3064−3066.
(59) Johnson, J. A.; Finn, M. G.; Koberstein, J. T.; Turro, N. J. *Macromolecules* **2007**, *40*, 3589−3598.
(60) Kloxin, A. M.; Kasko, A. M.; Salinas, C. N.; Anseth, K. S. *Science* **2009**, *324*, 59−63.
(61) Zhao, H.; Sterner, E. S.; Coughlin, E. B.; Theato, P. *Macromolecules* **2012**, *45*, 1723−1736.
(62) Laurent, B. A.; Grayson, S. M. *J. Am. Chem. Soc.* **2006**, *128*, 4238−4239.
(63) Bielawski, C. W.; Benitez, D.; Grubbs, R. H. *J. Am. Chem. Soc.* **2003**, *125*, 8424−8425.
(64) Veksli, Z.; Andreis, M.; Rakvin, B. *Prog. Polym. Sci.* **2000**, *25*, 949−986.

(65) Jeschke, G. *Macromol. Rapid Commun.* **2002**, *23*, 227−246.
(66) Helms, B.; Guillaudeu, S. J.; Xie, Y.; McMurdo, M.; Hawker, C. J.; Frechet, J. M. J. *Angew. Chem., Int. Ed.* **2005**, *44*, 6384−6387.
(67) Lee, C. C.; Gillies, E. R.; Fox, M. E.; Guillaudeu, S. J.; Frechet, J. M. J.; Dy, E. E.; Szoka, F. C. *Proc. Natl. Acad. Sci. U.S.A.* **2006**, *103*, 16649−16654.
(68) Peer, D.; Karp, J. M.; Hong, S.; Farokhzad, O. C.; Margalit, R.; Langer, R. *Nat. Nanotechnol.* **2007**, *2*, 751−760.